Escola de Primavera de Transição e Turbulência
Blumenau 2020

ABCM Associação Brasileira de Engenharia e Ciências Mecânicas

12th Spring School on Transition and Turbulence
September 21st-25th, 2020, Blumenau, SC, Brazil

# EPTT-2020-0115
# COMPARISON BETWEEN CFD MODELS COUPLED TO AN ACOUSTIC PRESSURE MODEL TO REPRESENT GAS-SOLID FLOWS IN A CFB RISER UNDER THE INFLUENCE OF ULTRASOUNDS

**Vivien Rossbach, Dr.**
Federal University of Santa Catarina (UFSC) - Campus Universitário, s/n - Florianopolis - SC, Brazil
University of Blumenau – Rua São Paulo, 3250 - Blumenau - SC, Brazil
vivienrossbach@gmail.com

**Sarah Laysa Becker, Me.**
**Natan Padoin, Dr.**
Federal University of Santa Catarina (UFSC) - Campus Universitário, s/n - Florianopolis - SC, Brazil
sarahlaysa@gmail.com, natan.padoin@ufsc.br

**Henry França Meier, Dr.**
University of Blumenau - Rua São Paulo, 3250 - Blumenau - SC, Brazil
meier@furb.br

**Cintia Soares, Dr.**
Federal University of Santa Catarina (UFSC) - Campus Universitário, s/n - Florianopolis - SC, Brazil
cintia.soares@ufsc.br

***Abstract***. *Ultrasonic waves applied in CFB risers can improve gas-solids mixture in the radial direction, which is necessary to improve phase contact in chemical processes. CFD models are widely used to represent gas-solid flows in CFB risers and the acoustic field generated in the gas flow can be obtained using the LES approach. In this study, k-$\varepsilon$ and Reynolds stress (RSM) turbulence models, Gidaspow and EMMS drag models were used to describe the gas-solid flow in a lab-scale CFB riser subject to an acoustic field with a frequency of 40 kHz and an input power of 10 W. The acoustic field was obtained for the gas flow at a velocity of 8.3 m/s without particles using LES and RANS approaches. RSM and k-$\varepsilon$ models combined with the EMMS model have a good agreement with the experimental data of solid velocity and volume fraction. The k-$\varepsilon$/EMMS model was chosen because of its lower computational cost. The pressure profiles in front of the transducers in the stagnant medium are different using k-$\varepsilon$ and LES models and it explains the pressure drop with the k-$\varepsilon$ model higher than in experiments. The results show that the solids flow impact the acoustic field and the RANS approach can be used to represent the gas-solid flow subject to an acoustic field.*
***Keywords:*** *circulating fluidized bed (CFB), acoustic field, computational fluid dynamics (CFD), gas-solid dispersion.*

## 1. INTRODUCTION

Circulating fluidized beds (CFB) are employed in several industrial applications, such as fluid catalytic cracking (FCC) (Lopes et al., 2011), $CO_2$ and $SO_2$ reduction (Tsai et al., 2002), coal combustion and gasification (Yin et al., 2012). One difficulty faced in these processes is the poor contact between gas and solid phases, caused by the accumulation of particles on the riser walls, and by the formation of particle clusters. Using acoustic waves is an innovative alternative to disperse solid particles in the gas phase and increase the gas-solid contact (Rossbach et al., 2020). The simulation of this flow using computational fluid dynamics (CFD) techniques is a problem that involves multiple scales. More accurate models, a short time step keeping the Nyquist criteria, and a numerical mesh with refinement at levels lower compared to the acoustic wavelength (Knoop and Fritsching, 2014) are needed to represent the sound wave propagation in the gaseous medium. Also, wave propagation in the air produces an acoustic streaming movement that is similar to a turbulent jet (Lighthill, 1978) and capable of increasing the gas-solid dispersion. Many processes use ultrasound waves to produce this effect, and its propagation in the gaseous medium is quick compared to the velocity of the gas-solid flow (Rossbach, 2020).

The simulation of turbulent gas-solid flows in the presence of an acoustic field is a challenge because it must reproduce phenomena at different scales without an excessive computational cost. Rossbach et al. (2020) adopted an Eulerian-Eulerian approach with the k-epsilon turbulence model representing the gas phase turbulence and the Gidaspow model describing the drag force between phases. The time step employed in the simulations was larger than the

wavelength, but it allowed to examine the effect that the acoustic energy transferred to the fluid causes on the flow of the solid particles dispersed in it. A time step shorter than the inverse of double the frequency of the wave is necessary to capture the sinusoidal shape of the sound waves, according to the Nyquist criteria (Rossbach et al., 2020). Sajjadi et al. (2015) simulated the gas-liquid flow in a sonochemical reactor employing the k-epsilon turbulence model and an acoustic model proposed by Cai et al. (2009) and obtained results similar to the experimental ones. This acoustic model is based on Lighthill's (1978) analogy and assumes acoustic pressure as being the excess pressure to the fluid-dynamic pressure. At acoustic powers higher than $4\times10^{-4}$ W, the acoustic streaming movement generated by the action of Reynolds stresses takes on a shape analogous to that of a turbulent jet (Lighthill, 1978). Considering that an ultrasonic wave is strongly damped just in front of its source, practically all the acoustic momentum is transformed into fluid-dynamic momentum just in front of the face of the transducer. Thus, the acoustic streaming in the fluid can be represented by an analogous turbulent jet (Trujillo and Knoerzer, 2011).

Valdès and Santens (2000) investigated the influence of turbulent airflow in a steady state on the acoustic streaming, employing a source with a sound frequency of 400 Hz. The permanently turbulent airflow with a low Mach number did not disturb the longitudinal gradients of mean pressure associated with the acoustic streaming and the mean axial velocity profile of the flow was not substantially disturbed by the acoustic field generated by an emitter positioned in the axial direction of the duct. The results showed, however, that the sound field modifies the Reynolds stresses of the flow. These results suggest that a mathematical model able to solve Reynolds tensors, such as the RSM (Reynolds Stress Model) (Speziale, 1991), can further describe the interaction between turbulent flow and the acoustic field. When adopting the RANS approach, it is necessary to run drag models to evaluate the transfer of momentum between the gas and solid phases. In this way, the EMMS (Energy Minimization Multi-Scale) model, proposed by Yang et al. (2003) is a multi-scale model capable of predicting the formation of clusters (Rossbach et al., 2019).

The rigorous description of the different scales of phenomena involved in this problem requires the adoption of more accurate models. Zhu and Tang (2020) performed CFD-DEM simulations to describe the dynamics of microparticles in a fluidized bed subject to low-frequency sound waves and concluded that this numerical approach can predict the breaking of particle clusters by comparison with experimental data. In contrast, the LES approach is more often used to describe pulsating flows because it allows direct solutions of the large turbulence scales, while the small scales of the flow are modeled (Gui and Fan, 2009). Likewise, Han et al. (2016) used the LES model to investigate the effects of the acoustic field on a turbulent premixed flame and found good agreement with the experimental data in the prediction of vortex structures.

This study aims to verify the accuracy of turbulence and drag models under the Eulerian-Eulerian approach to simulate the gas-solid flow in a lab-scale CFB riser subjected to ultrasonic waves with a frequency of 40 kHz and an input power of 10 W. RSM and k-ε models were employed to describe the turbulence of the gas phase, whereas the Gidaspow and EMMS drag models were investigated to describe the transfer of momentum between gas and solid phases. The numerical results were compared to experimental data of solid velocity and volume fraction obtained in a lab-scale CFB riser. For a better understanding of how the gas-solid flow affects the acoustic field, we also studied the propagation of the acoustic waves in the gas flow and in the stagnant air using RANS and LES approaches.

## 2. MATHEMATICAL MODEL

### 2.1 Eulerian gas-solid model

In this study, the turbulence of the gas phase in the gas-solid flow was represented by the k-ε model (Rossbach et al., 2020) with enhanced wall-treatment (k-ε/EWT-ε) and by the RSM model (Reynolds Stress Model) (Speziale, 1991). These models were used with the RANS (Reynolds-Averaged Navier-Stokes) approach. The k-ε/EWT-ε model combines a two-layer approach with wall functions to improve the results of the k-ε model in the viscous sub-layer. In the region close to the wall the presence of the boundary layer lead the ε values to be more affected by the fluid viscosity (ANSYS Inc. (US), 2013). For this reason, the standard k-ε model was employed in the turbulent region of the flow and the Wolfshtein (1969) equation model is adopted in the wall region. The RSM turbulence model adopted in this investigation follows was that proposed by Gibson and Launder (1978). RSM model is suitable to represent the effects of rotation and rapid changes in flow produced by acoustic waves in a gaseous flow. For example, Valdès and Santens (2000) observed that the effect of an acoustic field on a turbulent flow changes the Reynolds tensors of the flow and this effect can be better visualized using the RSM model.

The momentum transfer between the phases was computed adopting the classic Gidaspow drag model (Gidaspow et al., 1992) and the EMMS (Energy Minimization Multi-Scale) model proposed by Yang et al., (2003). The Gidaspow model is a combination of the Wen and Yu model for diluted flows with the Ergun equation for dense flows. This drag model is often used to describe dense gas-solid flows (ANSYS Inc. (US), 2013) and does not predict the formation of particle clusters and the flow not fully developed at the riser inlet (Rossbach et al., 2019). On the other hand, the EMMS model represents the formation of particle clusters by dividing the bed into two phases, which are identified as the cluster phase and the diluted phase. The energy of each phase and the energy of its interface are combined to get the energy necessary for the suspension and transport of the pseudo-phases. After the total energy is minimized to optimize flow

structures, such as the size of the clusters, the fraction of clusters in the flow, and the slip velocity. The equations for the global drag force of the flow are derived from these parameters (Yang et al., 2003) and the model equations can be found in Rossbach et al. (2019).

The Eulerian gas-solid model and the boundary conditions used in the simulations are presented in Table 1. The Eulerian-Eulerian approach implies that the gas and solid phases are continuous and interpenetrating. Besides the models previously mentioned, the KTGF model (Kinetic Theory of Granular Flow) was applied to describe properties of the solid phase, such as granular temperature, turbulent viscosity, and pressure of solids. The granular temperature was calculated using the differential form of its equation. The parameters of this model employed in the present simulations can be found in Rossbach et al. (2016). The non-reactive gas-solid flow was simulated considering air at ambient conditions such as a gas phase and Geldart B glass-beads as a solid phase. The gas flow has a superficial velocity of 8.3 m/s and the mass flow of solids is equal to 2.88 kg/m²·s. As there were no experimental pressure measurements at the riser outlet and this differs from atmospheric pressure, inlet and outlet conditions were modified. As air is suctioned, we assumed constant atmospheric pressure in the riser inlet. At the outlet, a constant gas velocity equal to 8.3 m/s was set, which can be obtained in ANSYS FLUENT 15.0 © by applying a velocity inlet with a negative signal. The boundary conditions used on the walls were non slip for the gas phase and free slip for the solid phase. The pressure-velocity coupling was calculated using the PC-SIMPLE (Phase-Coupled SIMPLE) scheme.

Table 1. Eulerian gas-solid model, boundary conditions, and operating conditions of the simulations.

| | |
|---|---|
| Approach: | Eulerian-Eulerian |
| Turbulence models: | k-ε EWT- ε and RSM |
| Drag models: | Gidaspow and EMMS |
| Solid-phase properties: | KTGF |
| Acoustic model: | Sajjadi et al. (2015) |
| Timestep: | $1 \times 10^{-5}$ s |
| Gas-phase: | Air at ambient conditions |
| Solid-phase: | Glass beads ($\rho = 2450$ kg/m$^3$; $d_p = 80$ μm) |
| Boundary conditions: | No-slip (gas phase) and free slip (solid phase) |
| Inlet conditions: | Constant atmospheric pressure |
| Outlet conditions: | Velocity outlet equal to 8.3 m/s (velocity inlet equal to -8.3 m/s) |
| Solids mass flux: | 2.88 kg/m$^2 \cdot$ s |

### 2.2 Acoustic model

An acoustic field applied to a fluid produces acoustic streaming (Lighthill, 1978). The acoustic pressure is the pressure in excess relative to the fluid-dynamic pressure**.** Cai et al. (2009) used a similar model**,** which describes the acoustic pressure produced on the flow by plane waves. Sajjadi et al. (2015, 2017) simplified Cai's model by removing the dependence on the position from the equation and introducing the effect of the acoustic streaming on the flow as a pressure inlet condition applied in the transducers faces. This modification considers that attenuation effects are computed by the gas-solid Eulerian model. The pressure model produces in the air a compression-and-rarefaction effect analogous to that of an acoustic wave with the same frequency and input power, given by:

$$P(t) = -P_a \sin(\omega t). \tag{1}$$

The acoustic pressure in Eq. (1) is calculated as:

$$P_a = \sqrt{2\rho_g I_{US} c_0}, \tag{2}$$

where ω is the angular frequency [rad/s], $c_0$ is the sound velocity [m/s], equal to 346.2 m/s in the air at ambient conditions, and $I_{US}$ is the intensity of the ultrasound, given as the ratio between the power acoustic [W] and the face area of the transducer [cm²]. The sound velocity value in the air was adopted because the gas-solid flow in the CFB riser is diluted, with porosity greater than 0.999 or 99.9%. Equations (1) and (2) were implemented in the ANSYS FLUENT © 15.0 code through a UDF (User Defined Function) routine. Eq. (1) was inserted as a pressure input term on the face of each transducer, emitting a mechanical wave analogous to the acoustic wave with a frequency of 40 kHz and input power of 10 W. The computational code adds the variation of acoustic pressure obtained from Eq. (1) to the atmospheric pressure to get the total pressure in front of the transducers.

An attenuation coefficient was not used in the acoustic model. However, the attenuation of the wave is predicted through the Navier-Stokes equations of continuity and momentum. The effect of the gas phase properties on the acoustic streaming was taken into account in Equation (2) and the flow was assumed to be compressible. The effect of air viscosity

is included in the sound velocity in the medium (c). A time-step of 1×10-5 s was adopted in the simulations of the gas-solid flow and the gas flow. This time-step value was calculated using the Nyquist criterion, which defines the minimum time step necessary to capture the behavior of an acoustic wave in transient simulations as the inverse of double the frequency of the wave. With this time step, 5 s of transient mean gas flow at 8.3 m/s and gas-solid flow were gathered. The acoustic field in a stagnant medium was calculated with a time step equal to 6.25×10-7 s, which is corresponding to 1/4 of the wave period for the frequency of 40 kHz.

The gas flow without solid particles was simulated with an air velocity of 8.3 m/s and with stagnant fluid. Thus, it was possible to find out how the turbulent gas flow and the gas-solid flow modify the acoustic field. When it is necessary to catch small-scale flow structures, more accurate models are employed. These models have been extensively used in technological applications despite their higher computational cost, as they describe properly the impact of microscopic phenomena on macroscopic quantities. The LES approach completely solves small scales and models the large ones (Meier, 2010). Several authors show that the LES approach is satisfactory to obtain the acoustic field in a fluid medium (Bennaceur et al., 2016). In this way, the airflow was simulated with a velocity of 8.3 m/s and with stagnant air, in the absence of the solid phase, using the LES approach and the k-ε / EWT-ε model. Then, it was possible to check the implications of using the k-ε/EWT-ε model to simulate a flow subject to an acoustic field. In the LES approach, the small scales of turbulence were computed using the Smagorinsky (SGS) tensor model, which takes into account the effect of filtered sub-grid turbulence.

## 3. MATERIAL AND METHODS

The numerical simulations of this study were done employing the mathematical models described in the previous section. The geometry of the CFB riser is illustrated in Fig. 1-a, b. The riser is 2.667 m high and has an internal diameter of 0.104 m. The ambient air is suctioned through the gas inlet for an exhauster located after the gas and solids outlet. The solid particles are added through a lateral inlet with an internal diameter of 0.044 m and a 45° inclination, located 0.4 m above the gas inlet. Air and solids are collected at the outlet, where the air passes through a bag filter and the solid particles are delivered to a cyclone and recirculated in the riser (Rossbach et al., 2019). The gas and solids outlet has a 12° slope relative to the solids inlet. The ultrasonic device is shown in Fig. 1-c and is located 0.7 m above the gas inlet. Acoustic waves with a frequency of 40 kHz and input power of 10 W are produced by each of the 20 ultrasonic transducers, which are positioned face to face on the x and y axes stated in Fig. 1-a. Each vertical row has five transducers arranged at a distance of 0.003 m from each other and the total height of the array is 0.092 m. The transducers have an external diameter of 0.016 m and a height of 0.01 m.

The ultrasonic waves were generated using a device developed by Rossbach (2020), based on the ultrasonic device designed by Marzo, Barnes, and Drinkwater (2017). Square waves corresponding to sinusoidal waves with a frequency of 40 kHz are produced and transmitted to an H-L298n bridge. The H-L298n bridge amplifies the wave power and sends the electrical signal to the transmitter, to be converted into an acoustic signal. The electronic device is fed back by a power supply of 10 V connected to the H-L298n bridge, which supplies energy to the Arduino board by the 5 V port. A switch button attached to the system controls the transmission of acoustic waves in the CFB riser. Phase Doppler anemometry (PDA) technique was employed to acquire experimental measures of the gas-solid flow with and without acoustic waves. A Dantec Dynamics A/S anemometer was utilized to perform non-invasive, single-point optical measures of velocity, concentration, and diameter of the solid particles. The solid volume fraction is the product of the concentration measured with PDA at each position, corrected by the punctual phase validation ratio, and the volume of a particle with a Sauter mean diameter of 79.9 μm. Details of this measurement technique can be found in Rossbach et al. (2019). The 20 ultrasonic transducers were numbered as shown in Fig. 1-e to compare their pressure and velocity profiles. A non-uniform, block-structured hexa-mesh with 525,000 elements was adopted to perform the simulations. The region close to the wall was refined, resulting in y+ values less than 0.5, and the elements of the transducer region are smaller than the 8.65 mm wavelength. Details of the cross-section and the lateral region of the mesh are illustrated in Fig. 1-d.

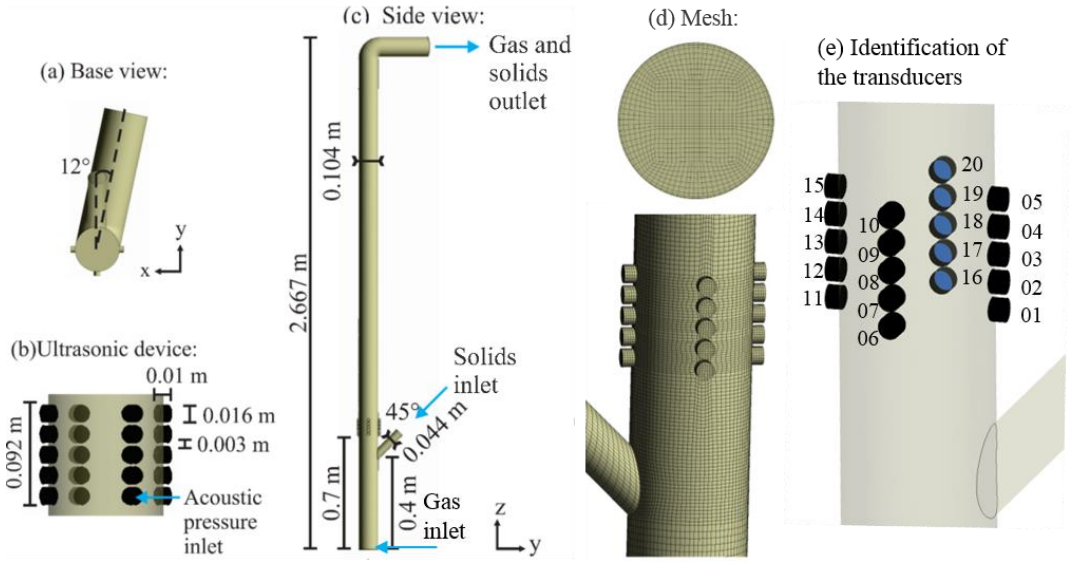


Figure 1. Geometry of the CFB riser: (a) base view of the gas and solids outlet; (b) ultrasonic device; (c) side view of the lab-scale CFB riser with the ultrasonic device; (d) Mesh properties.

## 4. RESULTS AND DISCUSSION

### 4.1 Comparison between CFD models and experimental results

As the main purpose of this study is to find a model capable of describing the gas-solid flow under the influence of acoustic waves, the gas-solid flow models were compared with experimental data gathered with the PDA technique. The comparison between the 4 combinations of turbulence and drag models and the experimental data is presented in Fig. 2. The solid velocity and volume fraction profiles were measured in the line perpendicular to the solids inlet drawn in the center of the duct, at 0.65 m above the gas inlet. The results illustrated in Fig. 2-a show that the k-ε/Gidaspow and RSM/Gidaspow models underestimate the solid's velocity. This result can be associated with the Gidaspow model since the velocity profile obtained with the RSM/EMMS model is closer to the experimental data. The Gidaspow model does not satisfactorily predict the formation of particle clusters that occurs near the wall and in the riser inlet region. The k-ε/EMMS model and the RSM/EMMS model present velocity profiles that are similar and close to the experimental data. If the RMS fluctuation of velocity is considered, the experimental data are within the range of values predicted by the k-ε/EMMS model at practically all positions. In the investigation of the solid volume fraction profiles, the k-ε/Gidaspow and RSM/Gidaspow models do not provide satisfactory predictions. In contrast, the k-ε/EMMS and RSM/EMMS models approximate to the experimental data, but the k-ε/EMMS model predicts a higher concentration of particles on the wall which is observed experimentally even with the use of the acoustic waves (Rossbach, 2020). Considering these results, the models k-ε/EMMS and RSM/EMMS can be chosen to describe the gas-solid flow under the influence of the acoustic field. Because of the high computational cost of the RSM model and the short time-step needed to describe the acoustic field, the k-ε/EMMS model was chosen.

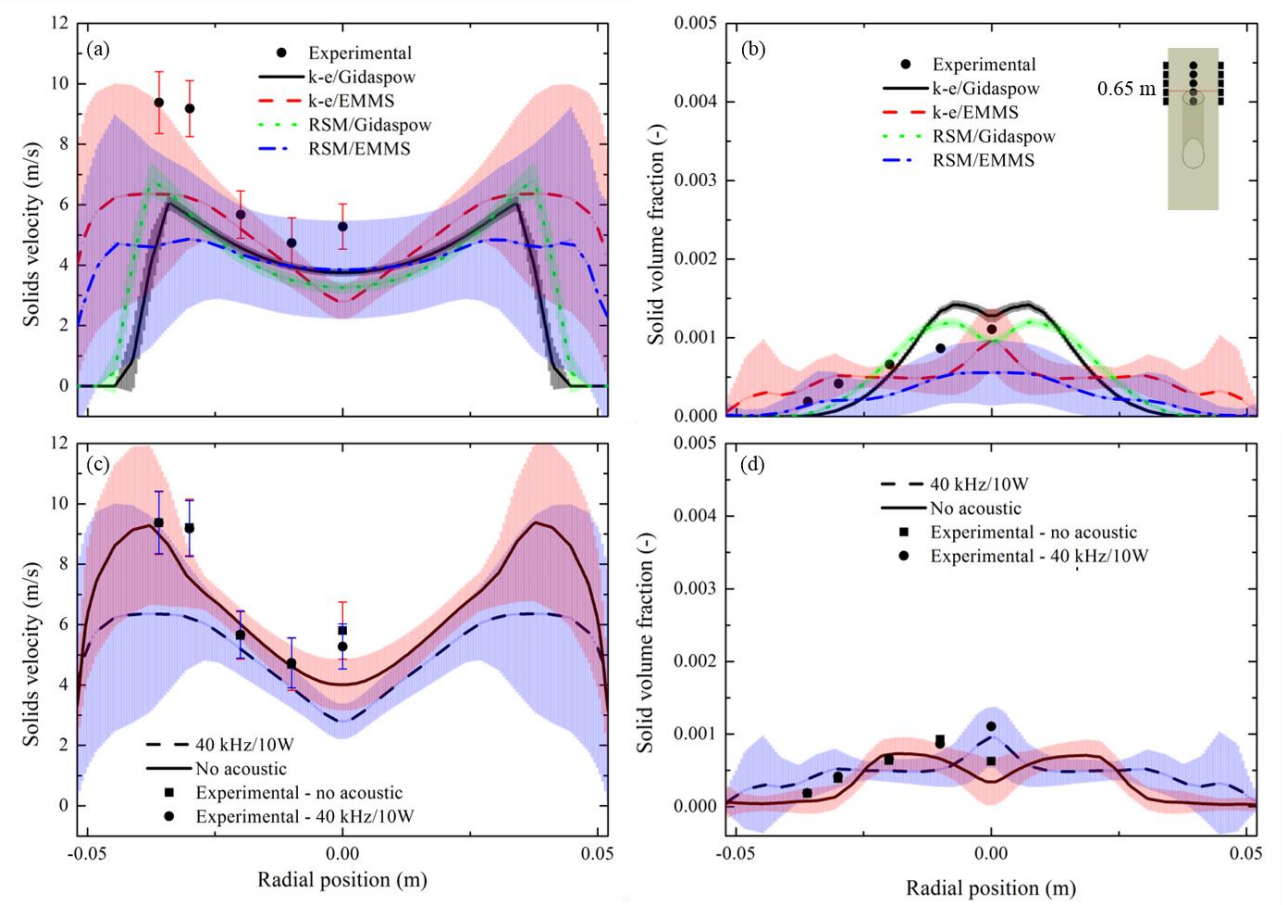


Figure 2. Comparison between CFD models and PDA data for (a) solid velocity and (b) solid volume fraction; comparison between k-ε/EMMS model and PDA data with and without acoustic waves: solid velocity (c) and solid volume fraction (d). bars refer to the RMS values of the variables.

In Fig.2-c,d, the solid velocity, and volume fraction profiles were compared in the flow with and without acoustic waves using the k-ε/EMMS model. In each case, the results were obtained over 5 s of transient mean flow using a time step of 1×10-4 s for the flow without acoustic waves and 1×10-5 s for the case with acoustic waves. RMS velocity and volume fraction was inserted in the charts as shadows and bars to indicate the fluctuation of the variables around their mean values in the transient simulations and the PDA measurements. The numerical profiles were also compared with the experimental data, showing notable variations only in the central region, where the solid velocity decreases, and its concentration rises with the use of the acoustic waves. The small difference observed in the profiles with and without acoustic waves can be related to the fact that the acoustic waves are emitted in the transversal direction of the riser and produce great variation in the radial velocity. Otherwise, the velocity component measured with PDA is the axial component. In the numerical velocity profiles, the axial velocity component was also set to be compared with the experimental results. Regarding the numerical results, there is a slight decrease in the velocity values and a more homogeneous distribution of solid particles along the cross-section with the acoustic waves, but with greater fluctuation. It is not possible to identify symmetric or unsymmetric behavior in the presented experimental data, but other studies (Rossbach et al., 2019, Lopes et al., 2011) show that the solid velocity and solid volume fraction profiles in a CFB riser tend to be axisymmetric.

The quadratic mean error (Spiegel and Stephens, 1998) and the Pearson correlation coefficient (Witz et al., 1990) were employed to perform a quantitative analysis of the results showed in Fig. 2-c,d, as indicated in Table 2. The RMS values were considered in this analysis to adjust the mean values. The values for the Pearson correlation coefficient demonstrate a high correlation between numerical and experimental data in the same points under the influence of acoustic waves. For the gas-solid flow without acoustic waves, a high to very high correlation was observed between numerical and experimental data. The quadratic mean error of the mean solid volume fraction was 3 orders of magnitude lower than the mean solid volume fraction values. For the solid velocity, the error is similar to the RMS values. The higher value of the mean quadratic error for the solid velocity was 2.327 in the case with acoustic waves. However, the visual analysis of the profiles in Fig. 2 indicates that the experimental values are within the margin of RMS values of the simulation. This higher error can be associated with the large velocity fluctuation near the wall.

Table 2. Comparison between numerical (CFD) and experimental (PDA) values of solid velocity and solid volume fraction with and without acoustic waves using the mean quadratic error (QME) and Pearson correlation coefficient ($r^2$).

| Radial position (m) | Solid volume fraction (-) | | | | Solid velocity (m/s) | | | |
|---|---|---|---|---|---|---|---|---|
| | No acoustic | | Acoustic | | No acoustic | | Acoustic | |
| | PDA | CFD | PDA | CFD | PDA | CFD | PDA | CFD |
| 0 | 0.001106 | 0.000439 | 0.000625 | 0.000586 | 5.28E+00 | 4.82E+00 | 5.81E+00 | 2.82E+00 |
| -0.01 | 9.25E-04 | 8.26E-04 | 8.64E-04 | 5.22E-04 | 4.69E+00 | 4.64E+00 | 4.74E+00 | 3.53E+00 |
| -0.02 | 6.35E-04 | 6.30E-04 | 6.60E-04 | 2.89E-04 | 5.65E+00 | 5.56E+00 | 5.67E+00 | 4.76E+00 |
| -0.03 | 3.89E-04 | 4.34E-05 | 4.15E-04 | 2.17E-04 | 9.21E+00 | 8.49E+00 | 9.18E+00 | 5.71E+00 |
| -0.036 | 1.84E-04 | 7.00E-07 | 1.89E-04 | 1.32E-04 | 9.37E+00 | 8.95E+00 | 8.27E-05 | 1.14E-04 |
| $r^2$ | 0.753 | | 0.799 | | 0.995 | | 0.938 | |
| QME | 6.080E-08 | | 2.987E-08 | | 0.092 | | 2.327 | |

Figure 3 shows the distribution of the solid volume fraction within the CFB riser and in the cross-sections in front of the transducers. In the absence of the acoustic field, the particles are preferably concentrated on the left side of the riser and near the wall, and its distribution has a constant behavior along the axial direction. With the use of the acoustic waves, the particles disperse radially, increasing its contact with the gas phase. There is a small accumulation of particles on the wall, much less than that observed in the case without acoustic waves. In the cross-sections in front of the transducers, the solids distribution keeps the shape of the acoustic field and its concentration in the center of the duct decreases with height. There is a region below the solids inlet where particles fall with acoustic waves, which can be induced by an increase in pressure drop in the transducer region and contributes to the reduction in the velocity noted in Fig. 2-c.

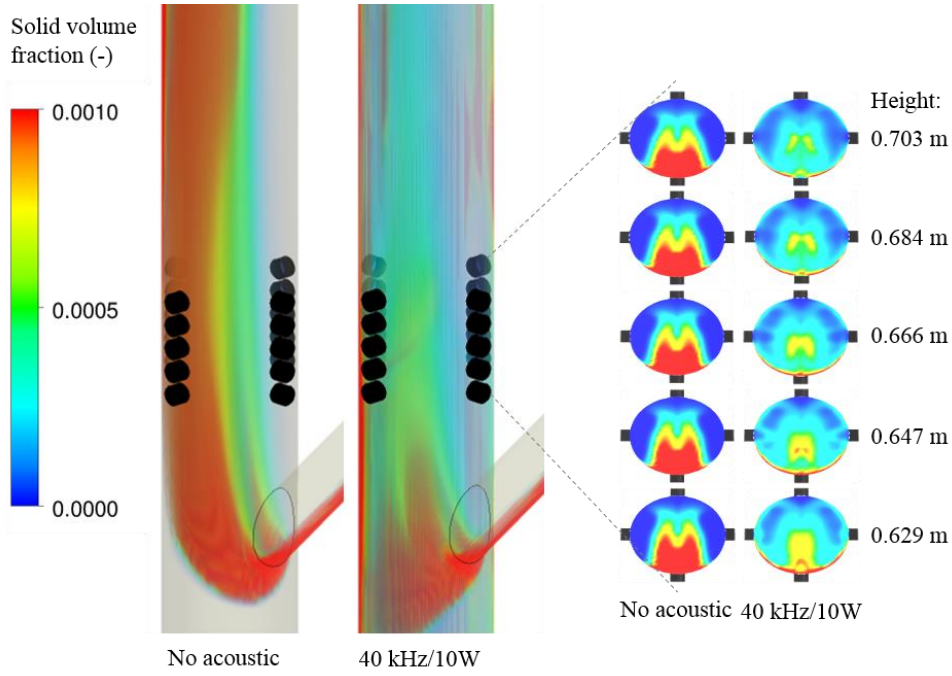


Figure 3. Solid volume fraction of the gas-solid flow without acoustic waves and with sound waves of 40 kHz and 10 W: isovolumes and cross-section contours in front of the transducers.

### 4.2 Comparison between the acoustic fields using LES and k-epsilon model

A more in-depth investigation of the acoustic field produced by the ultrasonic device in the riser is needed for a better understanding of the results of the gas-solid flow presented in the early section. For this purpose, gas flow simulations were carried out in the absence of solid particles and with stagnant fluid, to find out the influence of the gas turbulent flow and the solid phase flow on the acoustic field. Figure 4 shows the instantaneous pressure profiles on the riser with stagnant air. In these simulations, 4 timesteps were executed starting from the same initial state The time step

of 6.25×10-7 s used corresponds to a quarter of the wave period, to get the pressure variation over a period on the axis shown in Fig. 4-a. This position is at 0.629 m above the gas inlet, in front of the 4 lower transducers.

With the LES model, it is possible to identify a profile distinct from what is commonly encountered in the propagation of an acoustic field, with the displacement of the wave heights along with the distance in front of the transducer in a quarter of the wave period. In this case, mainly the increase of the wave height along the axial direction was observed. It can be caused by natural convection, however, in the short period analyzed, the strongest contribution is wave propagation since the natural convection is a slower phenomenon and a greater time of simulation is required to observe its effect. In the simulation with k-epsilon, it is not possible to identify differences in the acoustic wave profile in front of the transducers during a period T. On the contrary, the pressure profiles do not vary and overlap in the chart. Thus, the dispersion ratio of the acoustic field with a frequency of 40 kHz, analyzed along with the radial position and a period T, should be captured with the LES approach and not with the k-epsilon model. Also, the pressure peaks observed near the transducers are of the order of $7\times10^{-4}$ Pa with the k-epsilon model and $2\times10^{-7}$ Pa for the LES model. This contributes to justify why, in the simulation of the gas-solid flow with the k-epsilon model, the pressure drop in the transducer region leads to the fall of solid particles, which was not observed in the physical experiments conducted by Rossbach (2020). Despite the better acoustic field resolution obtained with the LES model, its use for solving the gas-solid flow takes a great computational cost. Thus, the k-epsilon model was employed. Despite the acoustic pressure field are higher than using the LES model, the k-epsilon model used in combination with the EMMS model provides results close to the experimental data for the distribution of solid velocity and volume fraction and can be used as an initial approximation for the gas-solid flow with acoustic waves.

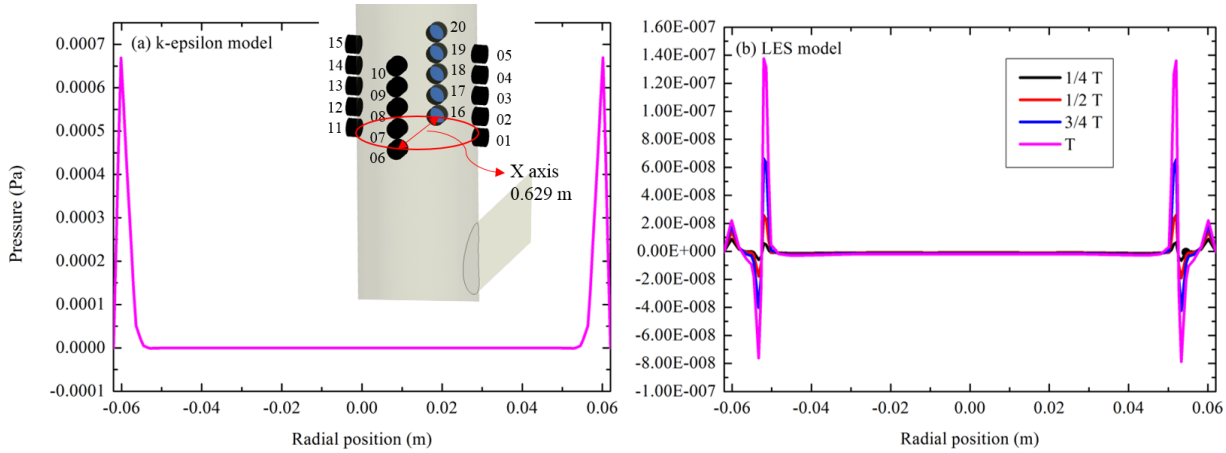


Figure 4. Pressure profiles using (a) k-ε model and (b) LES model for the gas phase. The pressure profiles are represented in front of the transducers rows at 0.629 m height, in the X-axis, at each 1/4 of the wave period.

Figure 5-a,b shows the absolute pressure profiles over the time in front of the 20 transducers in the gas flow, in the absence of the solid phase, using the LES approach and the k-ε/EWT-ε turbulence model. All simulations were done with a time step of $1\times10^{-5}$ s. A short phase difference is observed in the absolute pressure values between the transducers, but the pressure profiles are nearly the same for all. This phase difference can be associated with the slight asymmetry at the gas and solids outlet and with the interaction of the transducers with the gas pressure field and with the acoustic field of neighboring transducers. Figure 5-c shows the absolute pressure profiles of the gas-solid flow with time in front of the transducers. A zoom of this figure is shown in Fig 5-d for a further view of pressure fluctuations. The pressure difference and the oscillations remained as in the flow without solid particles. However, the absolute pressure values are different for each transducer or group of transducers. This takes place because of the asymmetry in the solids inlet adjacent to the ultrasonic device. In the single-phase flow there is a mean variation of 0.39 Pa relative to the atmospheric pressure of 101325 Pa using the k-epsilon. With the LES approach, this variation was 0.396 Pa. In the gas-solid flow, there was a mean variation of 75.5 Pa relative to atmospheric pressure. There is a mean decrease of 84 Pa between the lowest and the highest transducer in the rows perpendicular to the solids inlet. Also, there is a pressure difference of 72 Pa between the first and the last transducer in the row above the solids inlet. In the row opposite to the solids inlet, this decrease is about 70 Pa. Figure 6-a presents a comparison between the mean absolute pressure values in the gas-solid flow on the face of each transducer during 0.01 s of transient simulation. By observing the position of each transducer, it is possible to say that the absolute pressure decreases along with the height, generating a pressure drop in the riser that is greater in the two vertical rows of transducers perpendicular to the solids inlet. Most particles are concentrated near the wall in the row opposite to the solids inlet. Thus, gas pressure drop can damp by the solid particles in front of the transducers. In transducers 6 and 16, which are located perpendicular to the solids inlet, the pressure in the first transducer is higher and that of the last transducer is lower than in the rows parallel to this inlet.

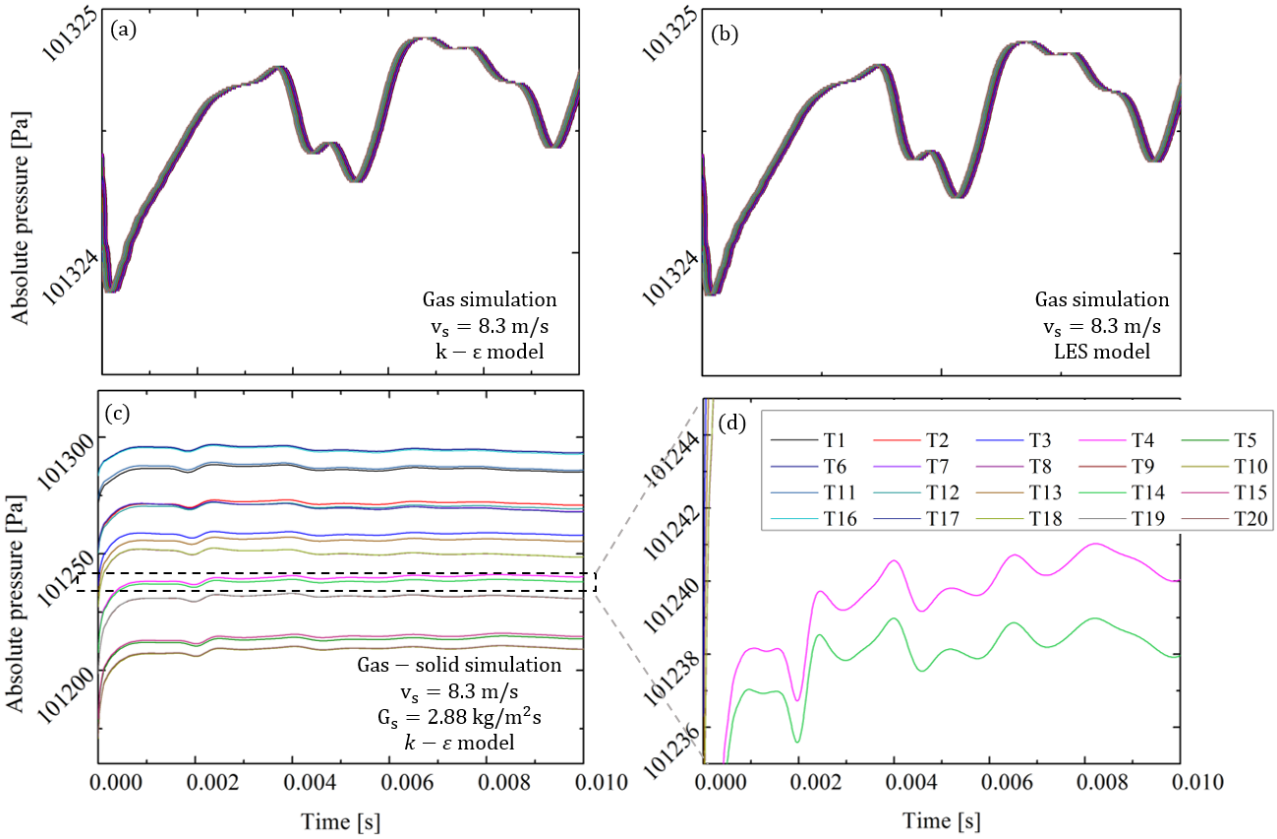


Figure 5. Absolute pressure profiles at the transducers' faces over time for gas flow with (a) k-$\varepsilon$ model, and (b) LES model; (c) absolute pressure profiles for the gas-solid flow using k-$\varepsilon$/EMMS model; (d) zoom of Fig. 2-c.

Figure 6-b,c illustrates the pressure distribution in the cross-sections in front of the transducers and the plane parallel to the solids inlet, respectively, for the single-phase flow with a velocity of 8.3 m/s at 3.34265 s and 3.34275 s of flow. This time interval is equivalent to 160 wave periods for a frequency of 40 kHz. There is a vertical and horizontal interaction between the acoustic fields of the neighboring transducers, generating regions of higher and lower pressure in the cross-section, which is caused by the compression-and-rarefaction movement produced in the air by the propagation of the acoustic wave. The region in the center of the duct and the set of transducers is where there is the greatest accumulation of pressure energy because of the propagation of acoustic waves, according to Fig. 6-c. The increase in pressure caused by the acoustic waves raise the radial velocity of the gas-solid flow, but if the input power of the transducers is higher, the pressure drop generated in the transversal region of the mean flow can lead to the fall of solid particles.

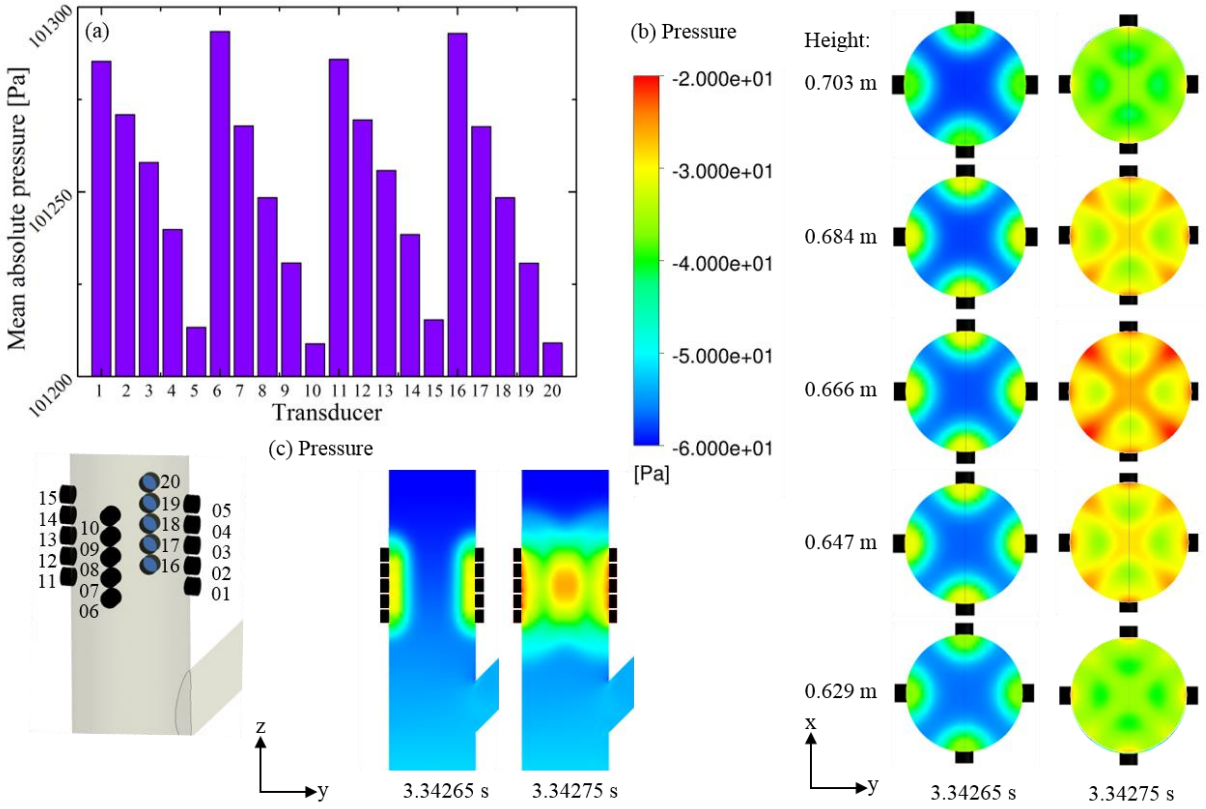


Figure 6. (a) Mean absolute pressure at the transducers; (b) instantaneous pressure in the cross-sections in front of the transducers and (d) along the riser at 3.34265 s and 3.34275 s using LES model ($v_g$ = 8.3 m/s).

## 5. CONCLUSION

In this paper, 4 CFD models using the RANS approach were compared to check whether they reproduce the behavior of gas-solid flow under the influence of acoustic waves. The simulations employing the EMMS drag model produced better results compared to the Gidaspow model, as the EMMS predicts the development of particle clusters in the CFB riser inlet region. The k-ε EWT-ε / EMMS model was chosen to describe the gas-solid flow under the influence of acoustic waves because it presented results similar to those obtained with the RSM / EMMS model and has a lower computational cost. A quantitative analysis of the flow with and without acoustic waves was performed by comparing the results obtained with the k-ε EWT-ε / EMMS model and experimental data, identifying a strong correlation between the data. The flow with acoustic waves was simulated without the presence of the solid phase and with stagnant air, indicating the interaction of the gas flow with the sound field and its deformation caused by the solid phase flow. Instantaneous pressure values in front of the transducers were computed using LES and k-ε EWT-ε turbulence models and it was found that the pressure values obtained with the k-ε EWT-ε model are higher than those obtained with LES, which can lead to a higher pressure increment in the cross-section of the main flow using the k-ε EWT-ε. However, the analysis of the gas-solid flow showed that this model can predict the behavior of the flow under the influence of acoustic waves.

## 6. ACKNOWLEDGEMENTS

The authors are grateful for the financial support of this research from the National Council for Scientific and Technological Development (CNPq), under process number 308714/2016-4. This study was financed in part by the Coordenação de Aperfeiçoamento de Pessoal de Nível Superior - Brasil (CAPES).

## 7. REFERENCES

ANSYS Inc. (US), 2013. "ANSYS Fluent Theory Guide", Vol. Release 14. Canonsburg, PA.

Bennaceur, I., Mincu, D.C., Mary, I., Terracol, M., Larchevêque, L., Dupont, P., 2016. "Numerical simulation of acoustic scattering by a plane turbulent shear layer: Spectral broadening study". *Comput. Fluids*. 138:83–98.

Cai, J., Huai, X., Yan, R., Cheng, Y., 2009. "Numerical simulation on enhancement of natural convection heat transfer by acoustic cavitation in a square enclosure". *Appl. Therm. Eng.* 29:1973-1982.

Gibson, M.M., Launder, B.E., 1978. "Ground effects on pressure fluctuations in the atmospheric boundary layer". *J.*

*Fluid Mech.* 86(03):491–511.
Gidaspow, D., Rukimini, B., Ding, J., 1992. "Hydrodynamics of circulating fluidized beds: Kinetic theory approach". *7th Fluid. Conf.*
Gui, N., Fan, J., 2009. "Numerical simulation of pulsed fluidized bed with immersed tubes using DEM–LES coupling method". *Chem. Eng. Sci.* 64(11):2590–98.
Han, X., Yang, J., Mao, J., 2016. "LES investigation of two frequency effects on acoustically forced premixed flame". *Fuel*. 185:449–59.
Knoop, C., Fritsching, U., 2014. "Dynamic forces on agglomerated particles caused by high-intensity ultrasound. *Ultrasonics*. 54:763-769.
Lighthill, S.J., 1978. "Acoustic streaming". *J. Sound Vib.* 61(3):391–418.
Lopes, G.C., Rosa, L.M., Mori, M., Nunhez, J.R., Martignoni, W.P., 2011. "Three-dimensional modeling of fluid catalytic cracking industrial riser flow and reactions". *Comput. Chem. Eng.* 35(11):2159–68.
Marzo, A., Barnes, A., and Drinkwater, B.W., 2017. "TinyLev: A multi-emitter single-axis acoustic levitator". *Rev. Sci. Instrum.* 88(8).
Meier, H.F., 2010. "Introdução à turbulência em escoamentos multifásicos". In *Turbulência*, eds. SS Mansur, EDR Vieira, A da S Neto, pp. 95–160. Rio de Janeiro: ABCM. 7th volume.
Rahimi, M., Azimi, N., Parvizian, F., Alsairafi, A.A., 2014. "Computational fluid dynamics modeling of micromixing performance in presence of microparticles in a tubular sonoreactor". *Comput. Chem. Eng.* 60: 403-412.
Rossbach, V., 2020. *Influência de ondas acústicas sobre a dispersão de partículas em um leito fluidizado circulante gás-sólido*. Ph.D. thesis, Universidade Federal de Santa Catarina, Florianópolis.
Rossbach, V., Padoin, N., Meier, H.F., Soares, C., 2020. "Influence of acoustic waves on the solids dispersion in a gas-solid CFB riser: Numerical analysis". *Powder Technol.* 359:292–304.
Rossbach, V., Utzig, J., Decker, R.K., Noriler, D., Meier, H.F., 2016. "Numerical gas-solid flow analysis of ring-baffled risers". *Powder Technol.* 297:320-329.
Rossbach, V., Utzig, J., Decker, R.K., Noriler, D., Soares, C., et al. 2019. "Gas-solid flow in a ring-baffled CFB riser: Numerical and experimental analysis". *Powder Technol.* 345:521-531.
Sajjadi, B., Raman, A.A.A., Ibrahim, S., 2015. "Influence of ultrasound power on acoustic streaming and micro-bubbles formations in a low frequency sono-reactor: Mathematical and 3D computational simulation". *Ultrason. Sonochem.* 24:193–203.
Speziale, C.G., 1991. "Analytical Methods For The Development Of Reynolds-Stress Closures In Turbulence". *Annu. Rev. Fluid Mech.* 23(1):107–57.
Spiegel, M. R., Stephens, L. J., 1998. "Schaum's outline of theory and problems of statistics". 3. ed. [s.l.] McGraw-Hill.
Trujillo, F. J., Knoerzer, K., 2011. "Modeling the Acoustic Field and Streaming Induced by an Ultrasonic Horn Reactor". In: *Innovative Food Processing Technologies: Advances in Multiphysics Simulation*, pp. 233–64.
Tsai, M.Y., Wu, K.T., Huang, C.C., Lee, H.T., 2002. "Co-firing of paper mill sludge and coal in an industrial circulating fluidized bed boiler". *Waste Manag.* 22:439–42.
Valdès, L.C., Santens, D., 2000. "Influence of permanent turbulent air flow on acoustic streaming". *J. Sound Vib.* 230(1):1–29.
Witz, K. et al., 1990. "Applied Statistics for the Behavioral Sciences". *Journal of Educational Statistics*.
Wolfshtein, M., 1969. "The velocity and temperature distribution in one-dimensional flow with turbulence augmentation and pressure gradient". *Int. J. Heat Mass Transf.* 12:301-318.
Yang, N., Wang, W., Ge, W., Li, J., 2003. "CFD simulation of concurrent-up gas-solid flow in circulating fluidized beds with structure-dependent drag coefficient". *Chem. Eng. J.* 96(1–3):71–80.
Yin, S., Jin, B., Zhong, W., Lu, Y., Shao, Y., Liu, H., 2012. "Experimental research of gas-solid flow behaviors in pressurized circulating fluidized bed - I: Solid holdup distribution". *Dongnan Daxue Xuebao (Ziran Kexue Ban)/Journal Southeast Univ. (Natural Sci. Ed.* 42(2):308–12.
Zhu, L., Tang, Y., 2020. "Effects of acoustic fields on the dynamics of micron-sized particles in a fluidized bed". *Powder Technol.* 372:625–37.

## 8. RESPONSIBILITY NOTICE

The authors are the only responsible for the printed material included in this paper.